Polarization Issues in a Recent Sedimentation Environment

Jandyr M. Travassos(jandyr@on.br), Simone S. André (sandre@on.br), Observatório Nacional/MCT-ON.

Abstract

This work presents the preliminary results of a GPR survey done at Marambaia, RJ. Part of data acquisition gotten in the region will be presented, and will show to the result of multi polarization of a GPR section.

For they had been in such a way carried through measured with room transmitter-receiver configuration bistatic (two linearly polarized and two crossed polarization) and CMP. All the data was obtained with a Sensor&Software PE100, with antennas de 100 MHz. A flow of basic processing was applied: data editing, dewow, band-pass filtering and SEC gain.

It approximately has indication of a water table is below 20 m. The signal go well beyond 400 ns, is safe to state that a sea water intrusion would be found below 30 m if any.

The unusual configurations (crossed polarization) show successfully some applications, as to focus in distinct way, reflectors that are not in optimal position to be detected. Through the multi components it can be produced images of the subsurface for some directions without previous knowledge of the reflectors.

The reflectors modify the polarization of the incident field, causing a linear or circular dependence, in accordance with the structures that can according to be focusing for each polarization of antenna.

Introduction

Almost all GPR surveys are performed with a parallel-broadside configuration, also known as the bistatic co-polar configuration, with antennae perpendicular to profile. However it has been known for a while that different configurations can be successfully used in some applications (Annan, 2000). Figure 1 shows the field configurations that may be used in GPR data acquisition. The nomenclature of Figure 1 will be adhered to hereinafter.

Broadside B(.) and endfire E(.) configurations take advantage of the nearly linearly polarized electromagnetic waves parallel to the long axis of the antenna although they have different radiation characteristics from each other. Both cases have the best S/N ratio as transmitting (T) and receiving (R) antennas have the same polarization. The crossed-dipole antenna configuration X(.) will have the worst S/N ratio the polarization of T is perpendicular to R. As a matter of fact we should have null field at R as a result of a X(.) configuration on a uniform earth.

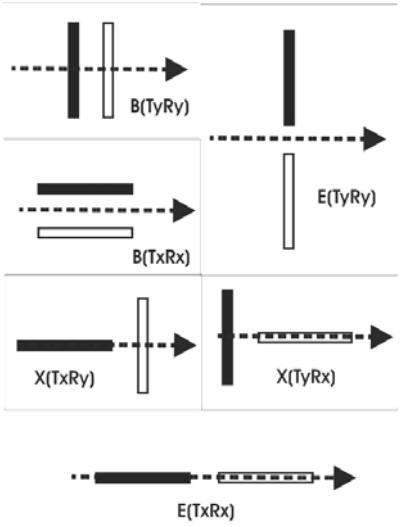

Figure 1. Antenna configurations that may be used in GPR data acquisition. T_i is the transmitting and R_i is the receiving antennae, the subscript indicating direction. Profile direction (x) is shown as a dash arrow. General configurations are broadside B(.), endfire E(.) and cross-polarization X(.). The broadside perpendicular (T_yR_y)is by far the most used field configuration for a bi-static GPR.

Many structures show high degrees of directionality, which are able to change field polarization. They can be either natural such as dipping beds or faults, or man-made such as a buried metallic pipe. As it will be illustrated in this work a dipping plane will give a different response whether the antennae are oriented parallel or perpendicular to the dip plane. Different antenna configurations may come into play as a focusing mechanism as in the case of depolarizing dipping bodies lying beneath obscuring flat-lying reflectors (Guy and Radzevicius, 1999). In this case a cross-dipole configuration may be the only configuration able to focus on structures below the flat-lying reflectors. Other application is to use a different antenna configuration to reduce the effect of a layer of many diffractors that obscure the later times (Travassos and Simões, 2004). As a rule an antenna configuration different from B(.) should be used when R does not record reflections from subsurface targets either due to a change the polarization of the incident wave or due to a highly scattering zone at earlier times.

The Data Set

The data set used in this work was acquired in Marambaia Isthmus the sand structure extended until length 40 km, the width varying of 120 m the 1800 m. It is used as a field of military training 30 km SW of the city of Rio de Janeiro. One is composed of fens, dunes, beaches and aluvial deposits. The Quartenary sediments form a transgress sequence that corresponds to an ascent of the level of the sea since 80 m below of the present level, during the interglacial period of training Riss-Würm. Figure 2 shows site location in the State of Rio de Janeiro.

We concentrate on a E-W profile of a GPR survey done in an area of 20 x 20 m in Marambaia Isthmus, as seen in Figure 2. All the data was obtained with a Sensor&Software PE100, with antenas de 100 MHz. We have used four field configurations: B(TyRy), B(TxRx), X(TyRx), and X(TxRy).

CMP profiles revealed a two-layer velocity model for the EM waves: [0 to 280 ns) $\rightarrow$ 0.14 m/ns; $\geq$ 280 ns $\rightarrow$ 0.09 m/ns. This indicates that the water table is below 20 m. As signal go well beyond 400 ns, is safe to state that a sea water intrusion would be found below 30 m if any.

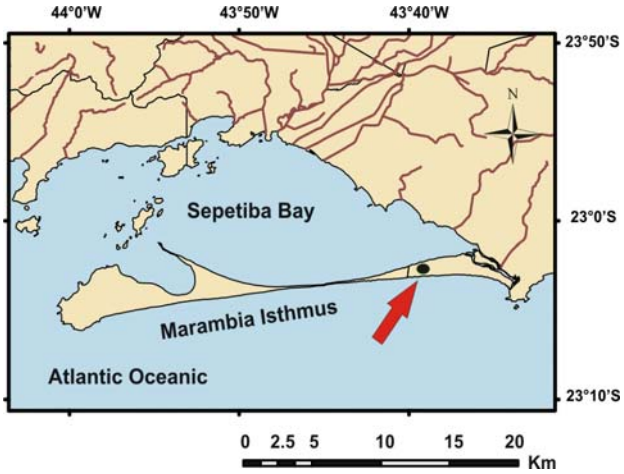

Figure 2. The Marambaia Isthmus in SW of the State of Rio de Janeiro. The study area location is shown as a black circle and it is arrowed to easy visualization.

Results

We have used a short processing flux: data editing, dewow, band-pass filtering and SEC gain. All figures below underwent the same processing. Depth penetration and S/N ratio are so good that we have signal down to almost 500 TWT.

Figures 3 to 6 show the results obtained for the polarizations B(TyRy), B(TxRx), X(TyRx), and X(TxRy).

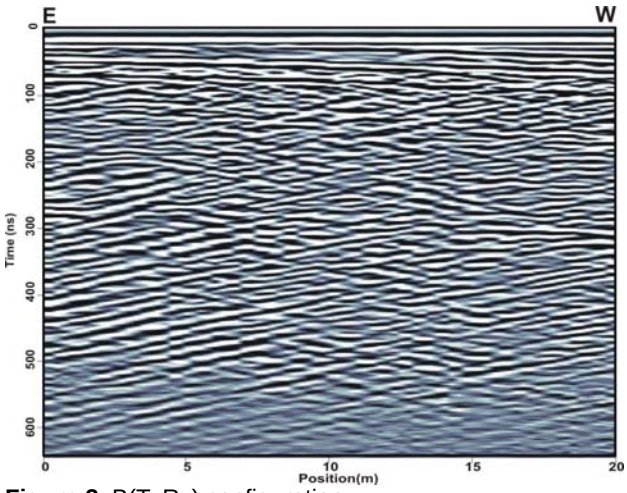

Figure 3. B(TyRy) configuration.

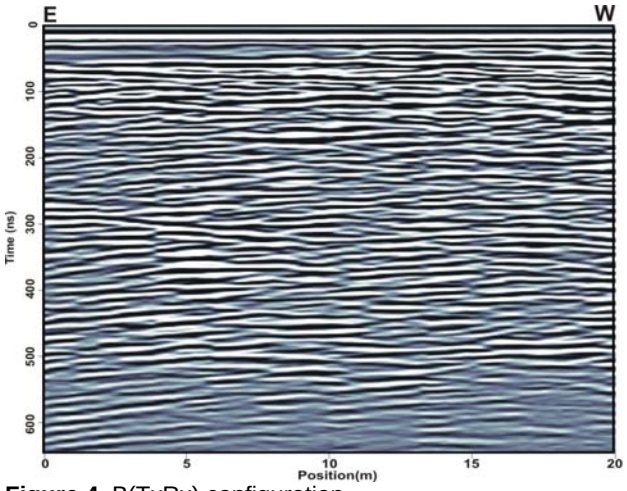

Figure 4. B(TxRx) configuration.

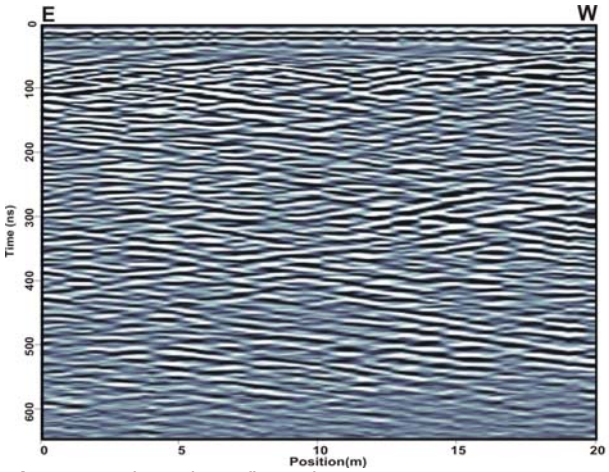

Figure 5. X(TyRx) configuration.

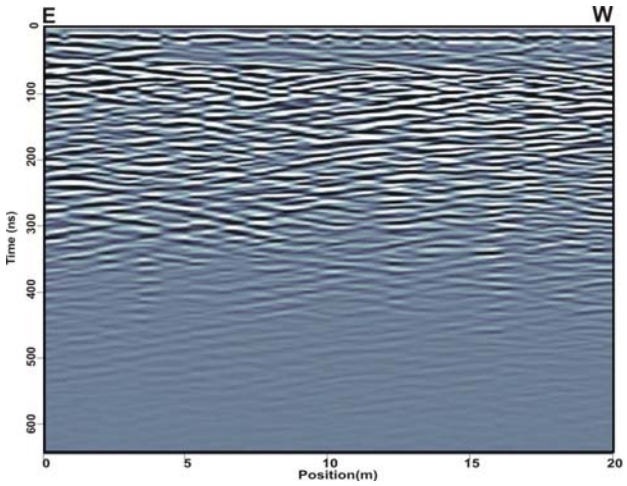

Figure 6. X(TxRy) configuration.

Figures 3 to 6 show the high degree of directionality of the dipping beds found in our study area. There are several dipping features only seen in the X(.) polarization, e.g., the feature between 300 and 400 ns and 5 and 10 m seen in Figure 5, 150 and 300 ns and 0 and 8 m seen in Figure 6 and nowhere else. That may be because the B(TyRy) antennae were oriented parallel or perpendicular to the dip plane. As the dipping plane polarize the incident waves the X(TyRx125) configuration is able to image the feature. Such an effect is better understood using a metallic cylinder, an extensively studied diffracting body. Metallic and low impedance cylinders are best imaged with the long axis of the antennae oriented parallel to the cylinder. If antennae are in angle with the long axis of the cylinder the polarization of incident waves change to a new direction with linear polarization, elliptical polarization, or circular polarization (Daniels et all., 2003; Kruk et al., 2003; Sassen and Everett, 2005).

The amplitude plots of a radargram are measurement of the instantaneous electric field intensity. The electric field intensity is a vector, having both magnitude and direction, therefore what the receiving antenna measures is the dot product of the electric field intensity and its orientation. In this way we can plot the magnitude of Rx versus Ry for a pair of any configurations. We can use the B(TyRy), B(TxRx) combination to illustrate this point as they have good S/N ratio. The radargrams in Figures 3 and 4 show more or less the same structures in the interval 30 – 55 ns. Those structures act on the polarization of the incident field approximately the same way resulting in a linear dependence between then as seen in the polarization plot shown in Figure 7. On the other hand the same radargrams show conspicuously different structures in the interval 255 – 310 ns. Those structures do change the polarization of the incident field in different way appearing as a circular dependence in the polarization plots as seen in Figure 8.

Conclusions

Multi-component GPR technique can provide a powerful imaging and discrimination capability that could be applied in studying sedimentary features with defined dips. It provides the interpreter with a number of combinations of antenna configurations and orientations that can be combined to give a more complete image of the subsurface.

Acknowledgements

One of the authors (SSA) acknowledges CAPES for a scholarship.

Bibliography

Annan, A.P. & Cosway, S.W., 1992, Ground Penetrating Radar Survey, Design, Annual Meeting of SAGEEP, Chicago, April, 26-29.

Annan, A.P., 2000, Workshop Notes, Sensors & Software Inc., 135p.

Daniels, J.J., Wielopolski, L., Radzevicius, S., and Bookshar, J., 2003, 3D GPR polarization analysis for imaging complex objects, in Proc. SAGEEP, San Antonio, TX, February, 2003.

Guy, E.D., Daniels, J.J., and Radzevicius, S.J., 1999, Demonstration of using crossed dipole GPR antennae for site characterization, Geophys. Res. Lett, 26, pp. 3421-3424.

Kruk, J., Wapenaar, C.P.A., Fokkema, J.T.,Berg, P.M., 2003, Three-dimensional imaging of multicomponent ground-penetrating radar data. Geophysics, 68, 1241-1256.

Sassen, D.S., Everett, M. E., 2005, Multi-component ground penetrating radar for improved imaging and target discrimination, in Proc. SAGEEP, Atlanta, GA, 2005.

Travassos, J. M., Simões, J. C., 2004, High-resolution radar mapping of internal layers of a subpolar ice cap, King George Island, Antarctica, Pesquisa Antártica Brasileira (Brazilian Antarctic Research), publ. Brazilian Academy of Sciences, vol. 4, 57-65.

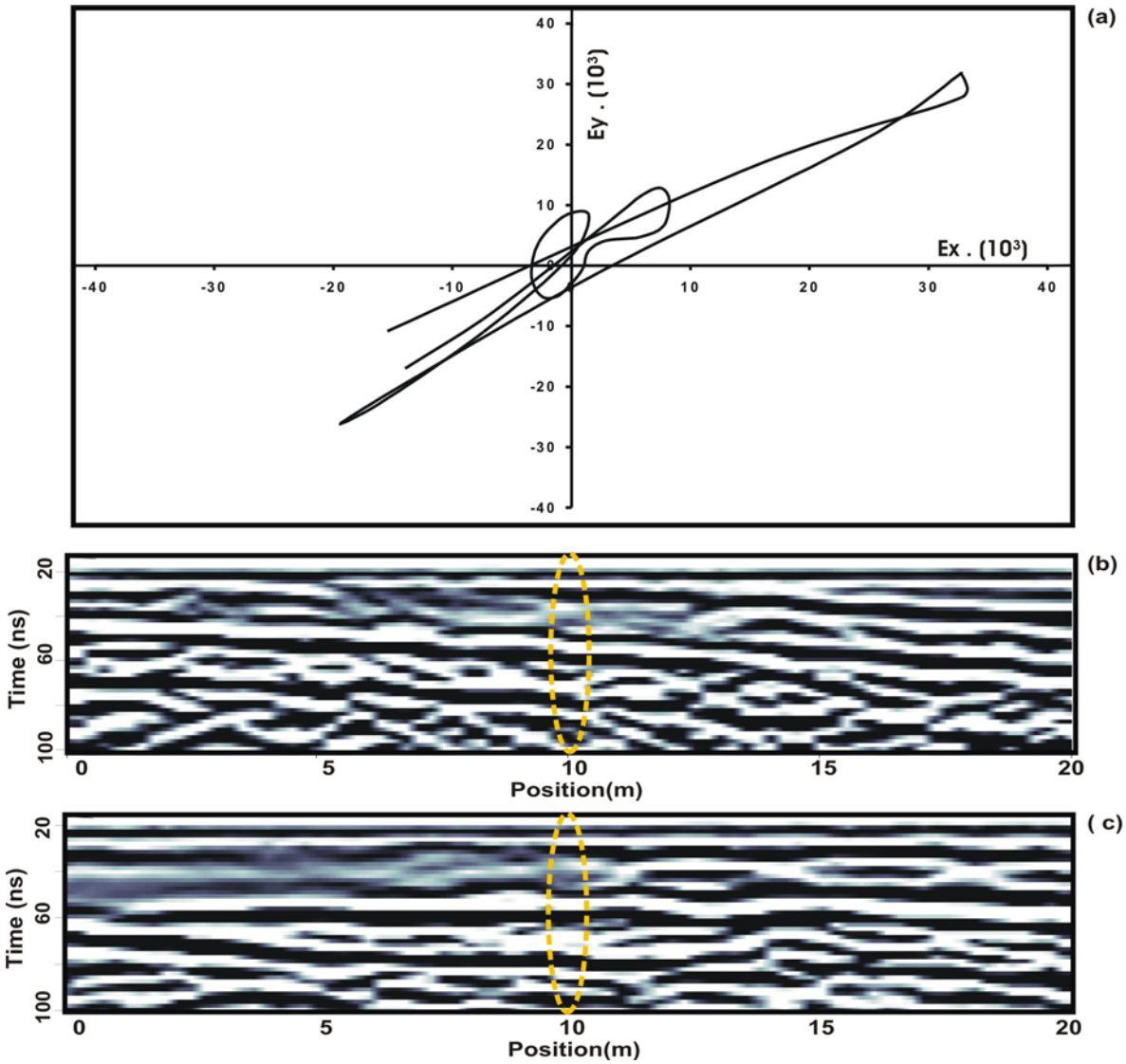

Figure 7. Polarization plot of Rx versus Ry for the B(TyRy) - B(TxRx) combination in the interval 30 – 55 ns for trace at 10 m (a). The two lower panels show the radargrams for the configurations B(TyRy), panel (b) and B(TxRx), panel (c). The trace at 10 m is in the center of the ellipse in yellow.

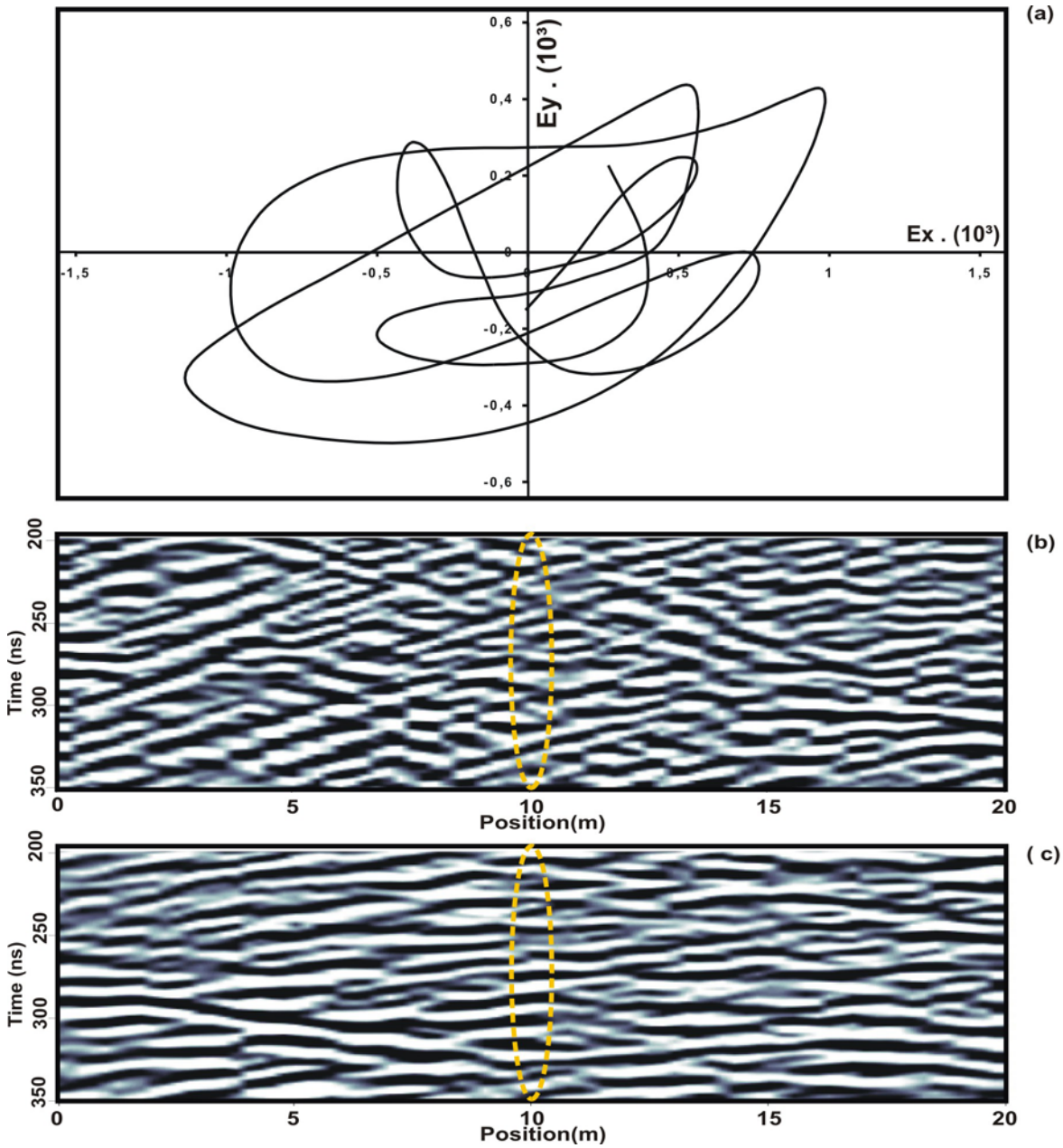

Figure 8. Polarization plot of Rx versus Ry for the B(TyRy) **-** B(TxRx) combination in the interval 255 – 310 ns for trace at 10 m (a). The two lower panels show the radargrams for the configurations B(TyRy), panel (b) and B(TxRx), panel (c). The trace at 10 m is in the center of the ellipse in yellow.